THE JOURNAL OF BIOLOGICAL CHEMISTRY Vol. 271, No. 32, Issue of August 9, pp. 19232–19237, 1996
Printed in U.S.A.

Regulation of the Kinetics of Phosducin Phosphorylation in Retinal Rods*

(Received for publication, September 13, 1995, and in revised form, April 16, 1996)

Jon F. Wilkins, Mark W. Bitensky, and Barry M. Willardson‡

From the Biophysics Group, Physics Division, Los Alamos National Laboratory, University of California, Los Alamos, New Mexico 87545

Phosducin (Pd) is a widely expressed phosphoprotein that regulates G-protein (G) signaling. Unphosphorylated Pd binds to G$\beta\gamma$ subunits and blocks their interaction with Gα. This binding sequesters G$\beta\gamma$ and inhibits both receptor-mediated activation of Gα and direct interactions between G$\beta\gamma$ and effector enzymes. When phosphorylated by cAMP-dependent protein kinase, Pd does not affect these functions of G$\beta\gamma$. To further understand the role of Pd in regulating G-protein signaling in retinal rod photoreceptor cells, we have measured the abundance of Pd in rods and examined factors that control the rate of Pd phosphorylation. Pd is expressed at a copy number comparable to that for the rod G-protein, transducin (G_t). The ratio of rhodopsin (Rho) to Pd is 15.5 ± 3.5 to 1. The rate of Pd phosphorylation in rod outer segment preparations was dependent on [cAMP]. $K_{½}$ for cAMP was 0.56 ± 0.09 μM, and the maximal rate of phosphorylation was ~500 pmol PO_4 incorporated/min/nmol Rho. In the presence of $G_t\beta\gamma$ this rate was decreased ~50-fold. From these data, one can estimate a $t_{½}$ of ~3 min for the rephosphorylation of Pd in rods during the recovery period after a light response. This relatively slow rephosphorylation of the Pd·$G_t\beta\gamma$ complex may provide a period of molecular memory in which sensitivity to further light stimuli is reduced as a result of sequestration of $G_t\beta\gamma$ by Pd.

Phosducin (Pd)[1] is a regulatory phosphoprotein that is expressed in many cell types (1–4). Pd regulates G-protein (G) signaling pathways by competing with Gα subunits for binding to G$\beta\gamma$ subunits (5). The efficacy of Pd binding to G$\beta\gamma$ is determined by its phosphorylation state (1, 5–7). Unphosphorylated Pd sequesters G$\beta\gamma$ and prevents receptor-mediated Gα activation (1, 5, 8). Binding of unphosphorylated Pd also blocks the direct interaction between G$\beta\gamma$ and effector enzymes (6, 7). When Pd is phosphorylated by cAMP-dependent protein kinase (PKA), it no longer affects these G$\beta\gamma$ functions (1, 5–7). Thus, the phosphorylation state of Pd determines the magnitude of G-protein-mediated signal amplification by regulating the availability of G$\beta\gamma$. Since many G-protein-linked pathways affect intracellular cAMP levels, and thereby affect PKA activity, Pd can serve as a feedback regulator of G-protein-mediated signal transduction.

In vertebrate rod photoreceptor cells, the photoresponse is mediated by a G-protein-linked pathway (reviewed in Ref. 9). Photon capture by rhodopsin (Rho) causes photoisomerization of its prosthetic group, 11-*cis*-retinal, to the all-*trans* isomer. This isomerization results in a conformational change that converts Rho to its active form, Meta II rhodopsin (Rho*). Rho* then binds to the retinal G-protein, transducin (G_t), allowing bound GDP to be exchanged for GTP on $G_t\alpha$. The released $G_t\alpha$-GTP then activates rod phosphodiesterase (PDE). Activated PDE lowers cytosolic cGMP concentrations, thereby closing the cGMP-gated cation channels in the rod plasma membrane. Closure of the cation channels results in hyperpolarization of the plasma membrane, thereby generating a neural impulse. Ion channel closure also reduces the flow of Ca^{2+} into the rod. Ca^{2+} continues to exit through a Na^+,K^+/Ca^{2+} exchanger, causing the cytosolic Ca^{2+} concentration to fall in response to light.

Rod cells can readily adjust their sensitivity to ambient light conditions and respond to photon fluxes spanning 3 orders of magnitude. Fully dark adapted rods have single-photon sensitivity. In this regime, a single Rho* can initiate hydrolysis of ~10^6 molecules of cGMP. With protracted or repeated exposure to light, however, this amplification mechanism is dramatically down regulated. Light adaptation causes a decrease in both amplitude and duration of the response resulting from a given light signal (reviewed in Ref. 10). Light-dependent reactions that appear to contribute to light adaptation include phosphorylation of Rho and arrestin binding (11), activation of guanylyl cyclase (12), and dephosphorylation of phosducin (5). The light-induced fall in Ca^{2+} concentration appears to trigger these adaptive events (12–14).

There is a correlation between the phosphorylation state of Pd and the degree of light adaptation in the rod. Pd is phosphorylated in the dark and becomes dephosphorylated upon exposure to light (15). In the light the dephosphorylated Pd can bind to $G_t\beta\gamma$ and prevent the activation of G_t by Rho* (5, 8). The period during which Pd remains bound to $G_t\beta\gamma$ defines a light-adapted state that persists until Pd is rephosphorylated. We have examined the rates of phosphorylation of Pd, both free and complexed with $G_t\beta\gamma$. The results provide evidence that the Pd·$G_t\beta\gamma$ complex could encode a molecular memory in retinal rods. The duration of this memory results from the stability of the Pd·$G_t\beta\gamma$ complex and the relatively slow rate of its phosphorylation. It is also shown that Pd is present in sufficient quantities to significantly reduce the amount of available G_t. Thus, the properties of Pd suggest that it could play a fundamental role in light adaptation.

EXPERIMENTAL PROCEDURES

Western Blot Quantitation of Pd in ROS—The Pd concentration in ROS was determined by quantitative Western blot analysis. Pd was

* This work was supported by National Institutes of Health Grant EY 06816. The costs of publication of this article were defrayed in part by the payment of page charges. This article must therefore be hereby marked "*advertisement*" in accordance with 18 U.S.C. Section 1734 solely to indicate this fact.

‡ To whom correspondence should be addressed. Current address: Dept. of Chemistry and Biochemistry, Brigham Young University, Provo, Utah 84602. Tel.: 801-378-2785; Fax: 801-378-5474.

[1] The abbreviations used are: Pd, phosducin; G, G-protein; G_t, retinal rod G-protein, transducin; PKA, cAMP-dependent protein kinase; Rho, rhodopsin; Rho*, light-activated rhodopsin; PDE, phosphodiesterase; PAGE, polyacrylamide gel electrophoresis; ROS, rod outer segment(s); 8-Br-cAMP, 8-bromo-cyclic AMP; 8-Br-cGMP, 8-bromo-cyclic GMP.

isolated from dark-adapted bovine retinas (J. A. Lawson and W. L. Lawson, Lincoln, NE) by a previously described method (5). This Pd was >95% pure, as determined by SDS-PAGE. Ten-μl samples of known concentrations of Pd ranging from 0.1 to 0.5 μM were prepared. Concentrations were determined using Coomassie Plus and bicinchoninic acid protein assay reagents (Pierce). The agreement between assay methods was greater than 90%.

Intact ROS were also isolated from dark-adapted bovine retinas under infrared illumination by a previously described method (16). Intactness of the ROS was determined by comparing the rate of light-induced phosphorylation of Rho* by exogenously added [γ^{32}P]ATP before and after disruption with a 27-gauge needle and syringe. The rate of Rho* phosphorylation was inhibited 87.3 ± 2.3% (n = 3) in the intact ROS, indicating that most of the ROS remained intact. Rho concentrations in the ROS preparation were determined by dark/light difference spectroscopy using an extinction coefficient for Rho of 40,000/M at 500 nm. Ten-μl samples of ROS were prepared at a range of Rho concentrations from 1 to 5 μM. The Pd from five different ROS samples and five different purified Pd samples was isolated by SDS-PAGE on 0.75-mm 12% Laemmli gels (17). Proteins were transferred to nitrocellulose by electrophoresis (18) for 90 min at 200 mA, and the nitrocellulose was blocked by incubation for 1 h at 23 °C in a 5% w/w solution of nonfat powdered milk (Carnation). The blot was then washed twice in HBS (10 mM HEPES, pH 7.5, and 500 mM NaCl) and shaken for 3 h with a 1:500 dilution in HBS of a polyclonal rabbit antiserum to a Pd/β-galactosidase fusion protein (19) at 23 °C. The blot was washed three times with HBS containing 0.05% w/v Tween 20 detergent (HBS-Tween) by shaking for 5 min, then incubated with shaking for 1 h in a 1:500 dilution in HBS of a horseradish peroxidase-conjugated goat anti-rabbit-IgG antibody at 23 °C. The blot was washed in 100 ml three more times for 5 min each with shaking, first with HBS-Tween, second with HBS, and third with 50 mM sodium citrate, pH 5.0. The blot was developed (20) by placing it in 80 ml of 50 mM sodium citrate, pH 5.0, and then adding 60 mg of 4-chloronaphthol dissolved in 20 ml of methanol. Two ml of 3% H_2O_2 were then added, and the blot was swirled for ~2 min, immediately rinsed with H_2O, and allowed to dry.

The Western blots were photographed, and the negatives were analyzed with a densitometric scanner. The peak for each band was integrated, and this value was multiplied by the length of the band. This product gives a "volume" value for each sample. The volume values were plotted against the amount of Pd or Rho in the sample. Slopes were determined from the linear portion of the curves. The slopes of the two curves were then compared to produce a Pd:Rho ratio. Arrestin in the ROS was also quantified in an analogous manner as a control for retention of soluble proteins during isolation of the ROS.

Pd Phosphorylation with ROS PKA—The Pd concentration dependence of Pd phosphorylation by ROS PKA was determined by experiments carried out under infrared illumination. Pd purified from dark-adapted bovine retinas as described above was used as a substrate for phosphorylation because endogenous Pd from intact ROS showed little phosphorylation. This was probably because the endogenous Pd became dephosphorylated and bound to $G_t\beta\gamma$ during isolation of the ROS. In the complex with $G_t\beta\gamma$, Pd phosphorylation is inhibited 50-fold (see Fig. 5). Very little $G_t\beta\gamma$ would remain free to bind exogenously added Pd and could not significantly inhibit phosphorylation of exogenous Pd.

Intact ROS (20 μM Rho) were disrupted with a 27-gauge needle and syringe in phosphorylation buffer (20 mM HEPES, pH 7.5, 100 mM KCl, 2 mM $MgCl_2$, 1 mM dithiothreitol, and 0.2 mM EGTA). The disrupted ROS were then incubated with a known amount of Pd, 10 μM (saturating) 8-Br-cAMP, and 1 mM [γ^{32}P]ATP (~200 mCi/mmol) in a total volume of 10 μl of phosphorylation buffer at 25 °C. Phosphorylation was begun by the addition of [γ^{32}P]ATP and quenched after 10 s by addition of 4 μl of a 4-fold concentrate of Laemmli denaturing sample buffer. Pd was then isolated by Laemmli SDS-PAGE on 0.75-mm 12% gels (17). The Pd band was excised, and the ^{32}P was quantified in a scintillation counter. Initial rates of phosphorylation at the various concentrations of Pd were estimated from the amount of phosphorylation occurring in 10 s. Rates of Pd phosphorylation by ROS PKA were measured similarly in the presence of known amounts of $G_t\beta\gamma$, purified as described previously (5). This experimental format was also used in the presence of known amounts of IP-20, a specific peptide inhibitor of PKA (21).

The cyclic nucleotide dependencies of Pd phosphorylation were determined in an analogous experimental format under infrared illumination. Pd phosphorylation was carried out as above, with the Pd concentration fixed at 5 μM, and with known amounts of either 8-Br-cAMP or 8-Br-cGMP in the incubation mixture. Phosphorylation was quenched with denaturing buffer after 10, 15, 25, or 40 s of incubation. The Pd was isolated, and the incorporated ^{32}P was quantified as described above. Initial rates of phosphorylation were determined by fitting the data from the four time points to the equation $p = p_{max}^*(1 - \exp(-t^*V_0/p_{max}))$, where p is the amount of ^{32}P incorporated, t is the incubation time, and V_0 is the initial rate of phosphorylation.

Pd Phosphorylation with Purified PKA—The ability of $G_t\beta\gamma$ to inhibit phosphorylation of Pd by exogenous PKA was measured with purified components. $G_t\beta\gamma$ was purified as described above, and the purified catalytic subunit of bovine heart PKA was purchased from Fluka. Pd (1.5 μM) was incubated with 2 mM [γ^{32}P]ATP (~200 mCi/mmol) in the presence of varying amounts of $G_t\beta\gamma$ and PKA in phosphorylation buffer. Experiments were run at PKA activities of 0.125, 0.25, and 0.5 units/μl, as indicated by the supplier. Phosphorylation was started by the addition of [γ^{32}P]ATP in a reaction volume of 15 μl. The reaction was run at 23 °C for 6 min and then quenched by the addition of 5 μl of a 4-fold concentrate of Laemmli denaturing sample buffer. Pd was isolated from the quenched sample by SDS-PAGE. The Pd band was excised, and the incorporated ^{32}P was quantified in a scintillation counter.

RESULTS

Quantitation of Pd and Arrestin in ROS—To understand the role of Pd in the regulation of rod phototransduction, it is necessary to determine the amount of Pd expressed in ROS. Since Pd functions by sequestering $G_t\beta\gamma$, the two would have to be expressed at comparable copy number in the rod for Pd to function as a meaningful regulator of G_t. The quantity of Pd present in intact ROS preparations was determined by quantitative Western blots, as described under "Experimental Procedures." A photograph of one of the blots is presented in Fig. 1*A*, and the corresponding densitometry data are shown in Fig. 1, *B* and *C*. Pd was present at one Pd per 15.5 ± 3.5 Rho (n = 7). G_t has been reported as being present at approximately one G_t per 10 Rho (22–24). Pd is thus present in nearly equimolar amounts with G_t.[2]

The amount of arrestin was also quantified as a control to determine whether soluble proteins were retained in our intact ROS preps. Arrestin was found to be present at one arrestin per 5.0 ± 1.5 Rho (n = 6), indicating that few soluble proteins were lost during the isolation of the intact ROS. Previous determinations of arrestin concentration gave values of approximately one arrestin per 10 Rho (25–27). The quantities of Pd present in ROS make it a good candidate for a major regulatory role in visual signal transduction and underscore the importance of the mechanism of regulation of Pd phosphorylation.

Identity of the Endogenous ROS Kinase—Endogenous kinase from bovine ROS phosphorylates Pd at Ser[73], which is part of a consensus sequence for PKA phosphorylation (28). This is also the site which is phosphorylated by purified PKA (28), indicating that PKA is likely to phosphorylate bovine Pd *in vivo*. Furthermore, amphibian ROS kinase has been identified as PKA (29). We tested the possibility that PKA is also the kinase present in bovine ROS by using an inhibitor of PKA to block phosphorylation of Pd by the endogenous kinase.

[2] Coomassie Blue-stained gels of intact ROS prepared in this manner do not show a band where Pd migrates with an intensity equal to 1/16th of the Rho band (16). This apparent discrepancy between the quantitative Western blots and Coomassie Blue-stained gels is probably a result of poor staining of Pd with Coomassie Blue compared to Rho staining in SDS-PAGE. The binding of Coomassie Blue R or G to protein is proportional to the positively charged residues on the protein and its hydrophobicity (41). Pd is a very hydrophilic protein, whereas Rho is very hydrophobic. SDS is a similar molecule to Coomassie Blue in that both have negatively charged groups and hydrophobic moieties (41). Appropriately, the binding of SDS to Pd is significantly less than its binding to Rho. In SDS gels, Pd migrates more slowly than predicted by its molecular weight because of low SDS binding, and Rho migrates more rapidly than predicted by its molecular weight because of high SDS binding. The quantitative Western blot is superior to comparisons of Coomassie Blue stain intensity for determining Rho:Pd ratios because it avoids the ambiguities of quantitatively significant differences in the binding of the dye to the different proteins.

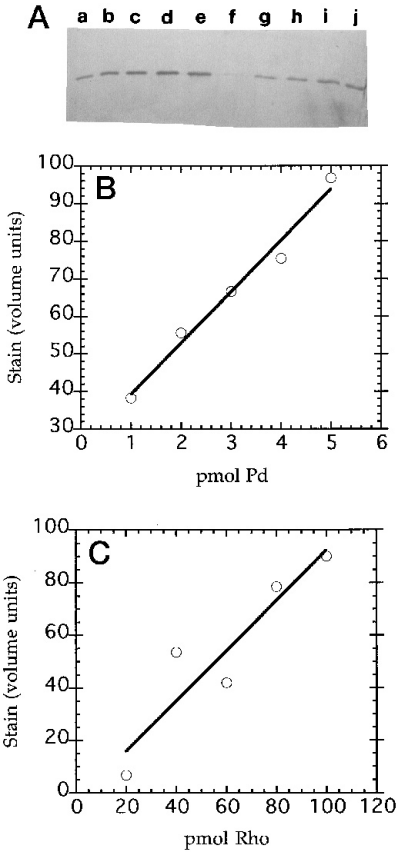

FIG. 1. **Quantification of Pd in ROS.** In *A*, Western blots were prepared and stained as described under "Experimental Procedures." *Lanes a-e* contain 1, 2, 3, 4, and 5 pmol of purified Pd, respectively. *Lanes f-j* show the stained Pd band from purified intact ROS and contain 20, 40, 60, 80, and 100 pmol Rho, respectively. In *B*, the extent of staining of the blot in each lane containing purified Pd was quantified as described under "Experimental Procedures." The *dashed line* represents the linear fit of the curve. The slope for this sample was determined to be 13.7 volume units/pmol Pd. In *C*, the extent of Pd staining in the ROS samples was determined as described in *B*. From these data, the slope is 0.96 volume units/pmol Rho. The ratio of the two slopes gives the Pd:Rho ratio. In this case, the ratio is 14.3 pmol Rho/pmol Pd. The average value from seven separate experiments was 15.5 ± 3.5 pmol Rho/pmol Pd.

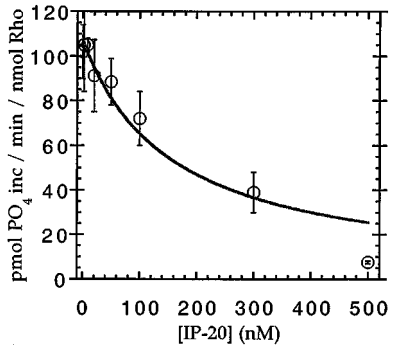

FIG. 2. **Inhibition of ROS endogenous kinase by IP-20 PKA inhibitor.** Rates of phosphorylation of Pd (5 μM) by ROS endogenous kinase were measured in the presence of the indicated concentrations of the IP-20 PKA inhibitor (20) as described under "Experimental Procedures." Measurements were carried out at 20 μM Rho in the presence of 10 μM 8-Br-cAMP. *Bars*, S.D. of the data from three separate experiments. The data were fit to the equation $V = V_{max}/(1 + ([IP\text{-}20]/K_{I1/2}))$, where V is the rate of Pd phosphorylation and $K_{I1/2}$ is the concentration of IP-20 at which half-maximal inhibition occurred. The curve fit yields a $K_{I1/2}$ value of 156 ± 37 nM.

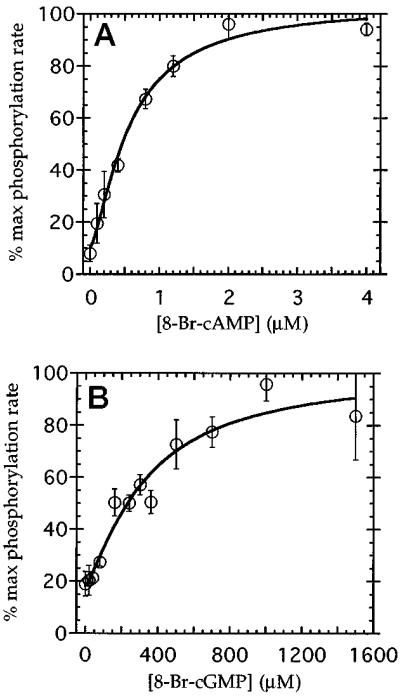

FIG. 3. **Cyclic nucleotide dependence of Pd phosphorylation.** Rates of Pd phosphorylation by ROS PKA were measured at the indicated concentrations of 8-Br-cAMP (*A*) or 8-Br-cGMP (*B*). The rate determination at any given nucleotide concentration was made by plotting out time dependencies of the phosphorylation as described under "Experimental Procedures." The experiments were performed at 20 μM Rho and 5 μM Pd. Each data point represents an average from three time curves ± the S.D. (*bars*). The maximal rate is 134 ± 26 pmol PO_4 incorporated/min/nmol Rho (n = 7). The curve fits of the data were generated with the Hill equation. The curve for the 8-Br-cAMP data gives a K_m of 0.56 ± 0.09 μM with an n_{app} of 1.4 ± 0.3. The curve for the 8-Br-cGMP data yields a K_m of 330 ± 115 μM and an n_{app} of 1.3 ± 0.5.

The data in Fig. 2 show the inhibition of Pd phosphorylation by the IP-20 peptide, which is specific for the α and β isoforms of PKA (30). Half-maximal inhibition occurred at a concentration of 156 ± 37 nM, and the data indicate complete inhibition at saturating concentrations of the peptide. This result confirms that PKA is the endogenous kinase responsible for Pd phosphorylation.

Endogenous Activation of ROS PKA—PKA is activated primarily by cAMP but can also be activated by cGMP at higher concentrations. In the dark-adapted state, ROS contain ~50 μM total cGMP (31–33) and ~5 μM total cAMP (34). Upon light-stimulated activation of the rod cell, the total concentration of both nucleotides drop by ~50% (31–35). The drop in free cAMP in ROS that results from light activation has not been measured, but free cGMP levels drop from ~5 μM to <1 μM (36). Both nucleotides have been considered as possible activators of ROS PKA. To understand the kinetics of Pd phosphorylation, it is important to determine which of the two activates PKA *in vivo*.

Pd phosphorylation by ROS PKA was measured at various concentrations of 8-Br-cAMP and 8-Br-cGMP (Fig. 3). The hydrolysis-resistant 8-bromo analogs were used to prevent inaccuracies resulting from PDE activity. No measurable hydrolysis of either nucleotide occurred over the course of the experiment (data not shown). Initial rates of phosphorylation were determined as described under "Experimental Procedures."

The dependencies of the initial rates of Pd phosphorylation for cAMP and cGMP are shown in Fig. 3. Half-maximal stimulation of the kinase with 8-Br-cAMP occurred at 0.56 ± 0.09 μM and exhibited a Hill coefficient of 1.4 ± 0.3 (Fig. 3*A*). This is consistent with two cooperatively interacting binding sites on

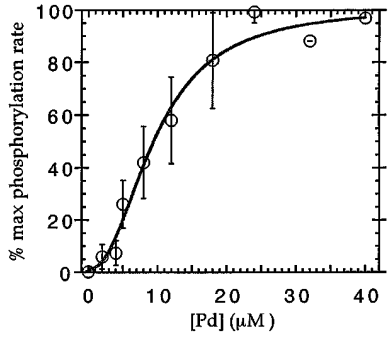

FIG. 4. **Effects of Pd concentration on the rate of Pd phosphorylation.** Rates of Pd phosphorylation by ROS PKA were measured at the indicated concentrations of Pd. Measurements were carried out at 20 μM Rho in the presence of 10 μM 8-Br-cAMP as described under "Experimental Procedures." *Bars,* the S.D. of the data from three separate experiments. The data were fit to the Hill equation, yielding a K_m of 9.7 ± 1.2 μM and showing a high degree of cooperativity (n_{app} = 2.2 ± 0.5). The maximal rate presented in this figure, based on the phosphorylation occurring in 10 s, is 390 ± 70 pmol PO_4 incorporated/min/nmol Rho (n = 3).

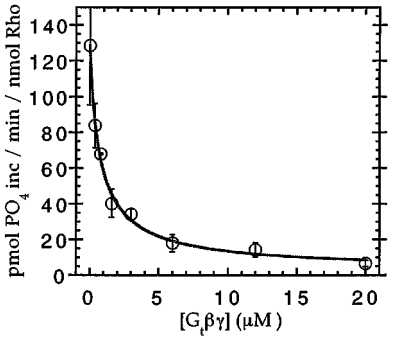

FIG. 5. **Inhibition of the phosphorylation rate of Pd by $G_t\beta\gamma$.** Rates of Pd phosphorylation by ROS PKA were measured in the presence of the indicated concentrations of $G_t\beta\gamma$. Measurements were carried out at 20 μM Rho and 1.5 μM Pd in the presence of 10 μM 8-Br-cAMP as described under "Experimental Procedures." *Bars,* the S.D. of the data from three separate experiments. The data were fit to the equation $V = ((V_{max} - V_{min})/(1 + ([G_t\beta\gamma]/K_{I1/2})^n) + V_{min}$, where V is the rate of Pd phosphorylation, n is a slope factor, and $K_{I1/2}$ is the concentration of $G_t\beta\gamma$ at which half-maximal inhibition occurred. The curve fit yields a $K_{I1/2}$ for the inhibition of 0.78 ± 0.11 and a slope factor of 0.93 ± 0.14. The values for V_{max} and V_{min} were determined to be 128 and 2.59 pmol PO_4 incorporated/min/nmol Rho, respectively. This corresponds to a 50-fold inhibition at saturating concentrations of $G_t\beta\gamma$.

each of the regulatory subunits of PKA (37). Fig. 3*B* shows that half-maximal stimulation by 8-Br-cGMP occurred at 330 ± 115 μM and was also cooperative (n_{app} = 1.3 ± 0.5). Activation by cGMP occurs in a range ~100-fold higher than the free concentrations present in ROS, making cGMP an unlikely candidate for the *in vivo* activator of ROS PKA. The range of PKA activation by 8-Br-cAMP, however, falls in a range over which free cAMP could vary *in vivo*.

These data indicate that cAMP is likely to be the activator of ROS PKA. Approximately 2 μM free cAMP is required to fully activate the kinase. Such concentrations of cAMP may be achievable in a dark-adapted rod. We estimate little or no loss of PKA in our intact ROS preparations, because other soluble proteins, Pd and arrestin, are retained. Therefore, the rates of phosphorylation that occur at maximal stimulation of the endogenous ROS PKA are reflective of the *in vivo* PKA concentration. This maximal rate was measured to be 134 ± 26 pmol PO_4 incorporated/min/nmol Rho (n = 7).

Dependence of Pd Phosphorylation Rate on Pd Concentration—The cAMP dependence of Pd phosphorylation was measured at 5 μM Pd. To get an accurate estimate of the *in vivo* phosphorylation rate, we measured the concentration dependence of Pd phosphorylation at saturating (10 μM) concentrations of 8-Br-cAMP. The experiments were carried out as described under "Experimental Procedures," and the data are shown in Fig. 4. The dependence was strongly cooperative (n_{app} = 2.2 ± 0.5) with the half-maximal rate occurring at 9.7 ± 1.2 μM Pd. Based on a Rho concentration of 6 mM in the interdiscal space (38) and the Pd abundance data presented above, we can estimate the concentration of Pd to be ~380 μM. Therefore, under physiological conditions the rate of phosphorylation would be fully saturated with respect to [Pd]. The maximal phosphorylation rate in the three sets of data shown in this graph, as estimated from the phosphorylation occurring in 10 s, is 390 ± 70 pmol PO_4 incorporated/min/nmol Rho. Due to the decrease in the rate that occurs as the pool of unphosphorylated Pd is diminished, this value may underestimate the phosphorylation rate at saturating Pd concentrations. The rate can be more accurately estimated by starting with the cyclic nucleotide dependence curves, since these rate data were constructed by curve fitting multiple time points to determine a true initial rate. At 5 μM Pd, the concentration at which the cyclic nucleotide dependence curves were generated, the phosphorylation rate is equal to 26 ± 9% of the rate at saturating [Pd]. Based on these data, the *in vivo* rate of Pd phosphorylation is 515 ± 178 pmol PO_4 incorporated/min/nmol Rho.

Inhibition of Pd Phosphorylation by $G_t\beta\gamma$—When Pd is dephosphorylated, it is found primarily in a complex with $G_t\beta\gamma$. Thus, the more significant rate of Pd phosphorylation is that measured in the presence of $G_t\beta\gamma$, a rate considerably slower than that for Pd alone. The extent of the inhibition by $G_t\beta\gamma$ was determined by running the phosphorylation experiments in the presence of increasing amounts of $G_t\beta\gamma$. The data presented in Fig. 5 show that half-maximal inhibition occurs at 0.8 ± 0.1 μM $G_t\beta\gamma$. The curve fit indicates that there is a 50-fold inhibition in the rate of Pd phosphorylation at saturating concentrations of $G_t\beta\gamma$. The rate of phosphorylation of the Pd·$G_t\beta\gamma$ complex would, therefore, be 10.3 ± 3.6 pmol PO_4 incorporated/min/nmol Rho. The presence of $G_t\beta\gamma$ showed no effect on the rate of phosphorylation of histone type III-S by PKA (data not shown), indicating that the inhibition of Pd phosphorylation is due to the interaction of $G_t\beta\gamma$ with Pd and not due to an interaction with PKA.

Mechanism of Pd Phosphorylation in the Presence of $G_t\beta\gamma$—These data raise the question of the nature of the inhibition of Pd phosphorylation by $G_t\beta\gamma$. The mechanism of inhibition determines whether the rate-determining step is the dissociation or the phosphorylation of the Pd·$G_t\beta\gamma$ complex. In a competitive model, the binding of $G_t\beta\gamma$ to Pd could completely block phosphorylation. The complex would have to dissociate to allow PKA to phosphorylate Pd. Alternatively, in a noncompetitive model, PKA could phosphorylate Pd while it is bound to $G_t\beta\gamma$, but at a slower rate than that for free Pd. This question was addressed in an experimental format with purified Pd and $G_t\beta\gamma$ and purified bovine heart PKA catalytic subunit (Fluka). $G_t\beta\gamma$ inhibition of Pd phosphorylation was measured at three different PKA activity levels. If $G_t\beta\gamma$ were a competitive inhibitor of Pd phosphorylation, one would expect all of the inhibition curves to show complete inhibition at saturating concentrations of $G_t\beta\gamma$. However, the curves shown in Fig. 6 each reach different levels of maximal inhibition. Since the addition of more PKA increases the rate of phosphorylation at maximal inhibition, PKA must be able to phosphorylate the Pd·$G_t\beta\gamma$ complex. This noncompetitive inhibition means that the K_m for the phosphorylation of the complex should be the same as that for free Pd. However, the maximal rate of Pd phosphorylation (V_{max}) in the complex will be 50-fold lower.

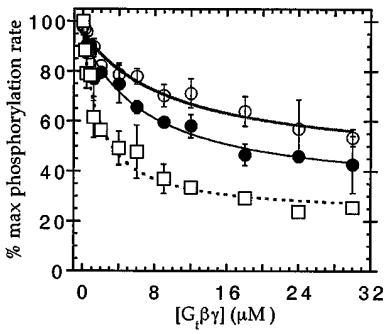

FIG. 6. **Inhibition of phosphorylation by $G_t\beta\gamma$ at different concentrations of PKA.** Rates of Pd phosphorylation by three different concentrations of PKA were measured in the presence of the indicated concentrations of $G_t\beta\gamma$. Purified bovine heart PKA (Fluka) was used at activity levels of 0.5 units/μl (○), 0.25 units/μl (●), and 0.125 units/μl (□), as indicated by the supplier. Measurements were carried out in the presence of 10 μM 8-Br-cAMP as described under "Experimental Procedures." *Bars*, the S.D. of the data from three separate experiments. The data from each curve were fit to the equation $V = ((V_{max} - V_{min})/(1 + ([G_t\beta\gamma]/K_{I1/2})) + V_{min}$, where V is the rate of Pd phosphorylation and $K_{I1/2}$ is the concentration of $G_t\beta\gamma$ at which half-maximal inhibition occurred. The values for V_{min} determined for the three curves were 43 ± 6%, 31 ± 6%, and 23 ± 3% of the maximum phosphorylation rate for the 0.5, 0.25, and 0.125 unit/μl samples, respectively.

DISCUSSION

Pd is expressed in many cell types that use G-protein-mediated signal transduction. Its ability to bind the $\beta\gamma$ subunits of G-proteins and to inhibit $G\beta\gamma$ functions raises questions regarding the nature of its role in signal regulation. We have shown that ROS PKA is activated *in vivo* by cAMP and not cGMP. Knowledge of the range and time scale of the changes in cAMP is thus crucial to a complete understanding of the regulation of Pd phosphorylation. The fall in cAMP that occurs upon light activation is the product of two events that result from light stimulation. Activated PDE will hydrolyze cAMP, albeit with a higher K_m than that for the hydrolysis of cGMP (39). Due to the large quantities of cGMP present in the ROS, cAMP may not undergo significant hydrolysis until the free cGMP levels have been sufficiently reduced. The ROS adenylyl cyclase also decreases its cAMP synthesis when Ca^{2+} levels drop following the closure of the cGMP-gated cation channels (14). Both of these events, therefore, require the drop in cGMP to occur before cAMP levels can decrease. The precise kinetics and magnitude of the cAMP decrease have not yet been measured. After cAMP levels fall and PKA is inactivated, the ROS phosphatase could act unopposed to dephosphorylate Pd.

Once Pd has become dephosphorylated, it is able to bind $G_t\beta\gamma$ and sequester it from $G_t\alpha$ (5), thus down-regulating subsequent G_t activation. The magnitude of this down-regulation is dependent upon the fraction of Pd that becomes dephosphorylated and forms a complex with $G_t\beta\gamma$. This correlates with the intensity and frequency of recent signaling events. At the ratio of 1 Pd per 16 Rho molecules reported here, sufficient Pd is present to sequester most of the $G_t\beta\gamma$ in ROS. Pd may thus modulate signal amplification in a manner commensurate with the recent signaling history of the rod.

One purpose of this study was to estimate the duration of the Pd-mediated light adaptation by determining the time scale for the rephosphorylation of Pd. Phosphorylation of Pd will not begin in earnest until Ca^{2+} levels have recovered, reactivating the ROS adenylyl cyclase, and the cyclase has had sufficient time to restore cAMP levels. The time following a light response required for the completion of these events is in the range of 1–5 s, as estimated from the turnover number of guanylyl cyclase of 60 μM/s at low (<50 μM) Ca^{2+} (12), the influx of Ca^{2+} through the cGMP-gated cation channels (10), and the turnover number of adenylyl cyclase of 1.7 μM/s at restored Ca^{2+} levels (>400 nM; Ref. 14). We have estimated the *in vivo* rate of the phosphorylation of the Pd·$G_t\beta\gamma$ complex by ROS PKA to be ~10.3 pmol PO_4 incorporated/min/nmol Rho. At a Pd concentration of ~380 μM in ROS, $t_{½}$ for the *in vivo* phosphorylation of Pd in the complex would be approximately 3 min. This $t_{½}$ is 10 times faster than the $t_{½}$ of 36 min for dissociation of the Pd·Gt$\beta\gamma$ complex, calculated from the dissociation rate constant of 3.2×10^{-4} s^{-1} (40). Furthermore, the data from Fig. 6 indicate that ROS PKA phosphorylates Pd·$G_t\beta\gamma$ and is not dependent on the dissociation of the complex to gain access to Pd. Phosphorylation of the complex thus appears to be a rate-determining step in the return of the rod to the dark-adapted state, which is characterized by large signal amplification.

The data were gathered using ROS preparations in which soluble proteins were retained; therefore, the measured phosphorylation rates should be a reasonable reflection of the *in vivo* PKA activity. Furthermore, under physiological conditions, the phosphorylation rate is saturated with respect to Pd and $G_t\beta\gamma$. The rate is dependent on the concentration of free cAMP, and those levels have yet to be measured; but under dark conditions in which PDE is inactivated and Ca^{2+} levels are high, the rate may be saturated with respect to cAMP as well. The rates presented here should, therefore, reasonably reflect the *in vivo* phosphorylation rates. Thus, mammalian rods may have a period of molecular memory, the duration of which is defined by a $t_{½}$ of ~3 min, in which light responses are down-regulated as a result of a persistent Pd·$G_t\beta\gamma$ complex.

Acknowledgments—We thank Drs. Che-Hui Kuo and Naomasa Miki (Osaka University School of Medicine, Osaka, Japan) for their generous gift of the polyclonal antibody to phosducin.

REFERENCES

1. Bauer, P. H., Müller, S., Puzicha, M., Pippig, S., Obermaier, B., Helmreich, E. J. M., and Lohse, M. J. (1992) *Nature* **358,** 73–76
2. Craft, C. M., Lolley, R. N., Seldin, M. F., and Lee, R. H. (1991) *Genomics* **10,** 400–409
3. Abe, T., Nakabayashi, H., Tamada, H., Tagaki, T., Sakuragi, S., Yamaki, K., and Shinohara, T. (1990) *Gene* (*Amst.*) **91,** 209–215
4. Kuo, C.-H., Taira, E., Takaha, N., Sohma, H., Akino, T., Fukada, Y., Sanada, K., and Miki, N. (1993) *Biochem. Biophys. Res. Commun.* **191,** 1097–1104
5. Yoshida, T., Willardson, B. M., Wilkins, J. F., Jensen, G. J., Thornton, B. D., and Bitensky, M. W. (1994) *J. Biol. Chem.* **269,** 24050–24057
6. Hekman, M., Bauer, P. H., Söhlemann, P., and Lohse, M. J. (1994) *FEBS Lett.* **343,** 120–124
7. Hawes, B. E., Touhara, K., Kurose, H., Lefkowitz, R. J., and Inglese, J. (1994) *J. Biol. Chem.* **269,** 29825–29830
8. Lee, R. H., Ting, T. D., Lieberman, B. S., Tobias, D. E., Lolley, R. N., and Ho, Y.-K. (1992) *J. Biol. Chem.* **267,** 25104–25112
9. Stryer, L. (1991) *J. Biol. Chem.* **266,** 10711–10714
10. McNaughton, P. A. (1990) *Physiol. Rev.* **70,** 847–883
11. Wilden, U., Hall, S. W., and Kühn, H. (1986) *Proc. Natl. Acad. Sci. U. S. A.* **83,** 1174–1178
12. Koch, K.-W., and Stryer, L. (1988) *Nature* **334,** 64–66
13. Kawamura, S. (1993) *Nature* **362,** 855–857
14. Willardson, B. M., Wilkins, J. F., Yoshida, T., and Bitensky, M. W. (1996) *Proc. Natl. Acad. Sci. U. S. A.* **93,** 1475–1479
15. Lee, R. H., Brown, B. M., and Lolley, R. N. (1984) *Biochemistry* **23,** 1972–1977
16. Schnetkamp, P. P. M., Klompmakers, A. A., and Daemen, F. J. M. (1979) *Biochim. Biophys. Acta* **552,** 379–389
17. Laemmli, U. K. (1970) *Nature* **227,** 680–685
18. Burnette, W. N. (1981) *Anal. Biochem.* **112,** 195–203
19. Kuo, C.-H., Akiyama, M., and Miki, N. (1989) *Mol. Brain Res.* **6,** 1–10
20. Hawkes, R. (1982) *Anal. Biochem.* **123,** 143–146
21. Cheng, H.-C., Kemp, B. E., Pearson, R. B., Smith, A. J., Misconi, L., Van Patten, S. M., and Walsh, D. A. (1986) *J. Biol. Chem.* **261,** 989–992
22. Baehr, W., Morita, E. A., Swanson, R. J., and Applebury, M. L. (1982) *J. Biol. Chem.* **257,** 6452–6460
23. Kühn, H., Bennett, N., Michel-Villaz, M., and Chabre, M. (1981) *Proc. Natl. Acad. Sci. U. S. A.* **78,** 6873–6877
24. Hamm, H. E., and Bownds, M. D. (1986) *Biochemistry* **25,** 4512–4523
25. Pfister, C., Chabre, M., Plouet, J., Tuyen, V. V., Dekozak, Y., Faure, J. P., and Kühn, H. (1985) *Science* **228,** 891–893
26. Bennett, N., and Sitaramayya, A. (1988) *Biochemistry* **27,** 1710–1715
27. Pfister, C., Chabre, M., and Kühn, H. (1983) *Eur. J. Biochem.* **136,** 489–499
28. Lee, R. H., Brown, B. M., and Lolley, R. N. (1990) *J. Biol. Chem.* **265,**

15860–15866
29. Hamm, H. E. (1990) *J. Gen. Physiol.* **95,** 545–567
30. Beebe, S. J., Salomonsky, P., Jahnsen, T., and Li, Y. (1992) *J. Biol. Chem.* **267,** 25505–25512
31. Woodruff, M. L., and Bownds, M. D. (1979) *J. Gen. Physiol.* **73,** 629–653
32. Cote, R. H., Biernbaum, M. S., Nicol, G. D., and Bownds, M. D. (1984) *J. Biol. Chem.* **259,** 9635–9641
33. Blazynski, C., and Cohen, A. I. (1986) *J. Biol. Chem.* **261,** 14142–14147
34. DeVries, G. W., Cohen, A. I., Hall, I. A., and Ferrendelli, J. A. (1978) *J. Neurochem.* **31,** 1345–1351
35. Blayzinski, C., and Cohen, A. I. (1984) *Exp. Eye Res.* **38,** 279–290
36. Nakatani, K., and Yau, K.-W. (1988) *J. Physiol.* **395,** 731–753
37. Taylor, S. S., Buechler, J. A., and Yonemoto, W. (1990) *Annu. Rev. Biochem.* **59,** 971–1005
38. Hargrave, P. A., and McDowell, J. H. (1992) *FASEB J.* **6,** 2323–2331
39. Miki, N., Baraban, J. M., Keirns, J. J., Boyce, J. J., and Bitensky, M. W. (1975) *J. Biol. Chem.* **250,** 6320–6327
40. Xu, J., Wu, D., Slepak, V. Z., and Simon, M. I. (1995) *Proc. Natl. Acad. Sci. U. S. A.* **92,** 2086–2090
41. Tal, M., Silberstein, A., and Nusser, E. (1980) *J. Biol. Chem.* **260,** 9976–9980